ESTIMATING AUSTRALIAN FOREST FIRE DANGER UNDER CONDITIONS OF DOUBLED CARBON DIOXIDE CONCENTRATIONS

TOM BEER
CSIRO Bushfire Unit, Mordialloc, Vic. 3195, Australia

and

ALLYSON WILLIAMS
Dept. Geography & Environmental Science, Monash University, Clayton, Vic. 3168, Australia

Abstract. The most appropriate indices with which to quantify Australian bushfire danger are the McArthur fire danger meters. These meters use meteorological information to produce a fire danger index that is directly related to the chance of a fire starting – and to the severity of a fire once it has started. The Mark 5 forest-fire danger meter uses air temperature, relative humidity and wind speed, plus a drought factor that is calculated using daily rainfall and temperature information.

Three years of daily data generated from the CSIRO four-level general circulation model, and thirty years of daily data generated from the CSIRO nine-level model were used to estimate the daily McArthur forest fire danger index for simulations corresponding to present conditions, and to those corresponding to doubled atmospheric CO_2. The performance of these models with respect to fire danger was tested by comparing the fire danger index for Sale (in the Eastern part of Victoria, South-eastern Australia) calculated from analysis of daily climatological data with the modelled annual cumulative forest fire danger index for the grid point that was representative of Sale. Data from both models for all Australian grid points were also examined. Both models predict an increase in fire danger over much of Australia for their doubled CO_2 scenarios.

The results from the models confirm that annually averaged daily relative humidity is the single most important variable in the estimation of forest fire danger on an annual basis, yet the models tend to produce relative humidities that are slightly too low so that the fire danger is overestimated. A simple one-box model of evaporation indicates that the value of relative humidity to be expected under an altered climatic regime depends on the modelled relation between actual and potential evaporation, the present values of relative humidity and evaporation rate, as well as on the expected changes in wind speed.

1. Introduction

One of the most dramatic manifestations of severe drought is the increased prevalence of wildfires, or bushfires as they are called in Australia. The Ash Wednesday fires of 16 February 1983, which were associated with the severe 1982/83 El-Niño Southern Oscillation event, were conflagrations of exceptional magnitude which killed 77 people and completely destroyed 2,528 homes. The recent fires that ringed Sydney during January 1994 received extensive international media coverage. As a result of many fires such as these, Australia has a 'fire-aware' community. Many state authorities have therefore expressed interest in the fire-regimes that could occur in a climate whose mean temperature has been increased as a result of greenhouse gas emissions.

The underlying physics controlling wildfire behaviour is poorly understood (Beer, 1991b) so that a study involving wildfire needs to use empirical models

Climatic Change **29:** 169–188, 1995.

whose validity is likely to be localised. Balling *et al.* (1992) correlated climate variables with annual area burnt in Yellowstone Park, whereas Fried and Torn (1990) and Torn and Fried (1992) use a Californian based fire modelling system to study climatic impacts on wildland fire. The most appropriate indices with which to quantify Australian bushfire danger are the ones that have received widespread acceptance by rural fire-fighting authorities throughout Australia. These are the McArthur fire danger meters for grasslands and forests (McArthur, 1966, 1967). During the summer months these meters are used on a daily basis to calculate fire danger indices that are directly related to the chance of a fire starting (Gill *et al.*, 1987), and once it exists, the forward speed, difficulty of suppression and, in combination with the fuel load, the intensity of the fire. These fire danger indices are calculated from meteorological information. The Mark 4 grassland fire danger meter, which is the simplest meter, uses air temperature, relative humidity, wind speed and degree of curing to produce a grassland fire danger index. The Mark 5 forest fire danger meter again requires air temperature, relative humidity, and wind speed but is also based on a drought factor (see Equation 2, below) with values ranging from 0 to 10. These meters have been calibrated in south-eastern Australia where they are widely used either in the form of cardboard nomographs, as a set of computational algorithms (Noble *et al.*, 1980), or in tabulated form (Beer, 1991a).

Beer *et al.* (1988) estimated the bushfire danger in Australia under an altered climatic regime (using an assumed scenario of a latitude dependent temperature change) by using archived weather data to calculate the annual sum of the daily values of the McArthur Forest Fire Danger Index (F). The grassland fire danger index was not considered because it is dependent on curing. Because grass curing depends on plant life cycles, its rate varies between species and with current climatic conditions. In practice, its value is estimated by observation – either by direct visual observation or by satellite remote sensing. There is no agreement on an objective procedure with which to model curing under present day climate. Weather-based mathematical models for estimating the development and ripening of crops have been reviewed by Robertson (1983) and it may be possible to construct a model of ripening based on the work therein. However curing involves the extra complication of plant senescence, for which there appears to be no acceptable mathematical model.

This article extends the analysis of Beer *et al.* (1988) using daily data produced by a three-year run of the CSIRO four-level general circulation model (GCM) (hereafter referred to as CSIRO4) and a thirty-year run of the CSIRO nine-level GCM (hereafter CSIRO9). Two cases were examined – the first simulating present climatic conditions, and the second simulating the case of doubled CO_2. This article follows the earlier paper in assuming that F is a valid quantification of forest danger in both present and future climates. Details concerning the GCMs may be found in Gordon (1981), Gordon and Hunt (1987) and McGregor *et al.* (1993). Both the four-level and nine-level models use a global grid (a rhomboidal truncation at 21 waves) such that there are 64 equally spaced east-west points, and 28 unevenly

spaced latitudes per hemisphere. The Australian continent is covered by 43 grid points spaced roughly 500 km × 500 km apart.

Whetton and Pittock (1991) examined seven general circulation models used in enhanced greenhouse experiments and found, at that time, the CSIRO4 model produced the most acceptable control simulation for Australia, and hence consider the CSIRO4 2 × CO_2 simulation as more likely to be a reliable guide to climatic change in the Australian region. In a more recent study that included the more recent CSIRO9 model, Whetton *et al.* (1994) found all five of the more recent GCMs that they examined produced adequate simulations of the present day climate. In general, CSIRO9 is more accurate than CSIRO4 in simulating the present climate. The major weakness of the CSIRO4 model is in its ability to simulate the Australian precipitation field. This is worrisome within the context of fire modelling because, as shown in this paper, the future behaviour of the hydrological cycle is crucial to understanding any future fire danger, and if this is not well simulated then inevitable uncertainties arise as to the validity of the results. To this extent any results obtained with the general circulation model need to be seen as interim – and subject to subsequent verification with more sophisticated modelling.

2. Forest-Fire Danger Index

The equation for the forest fire danger index, F, is (Noble *et al.*, 1980):

$$F = 1.275D^{0.987} \exp\left(\frac{T}{29.5858} - \frac{H}{28.9855}\right) \exp\left(\frac{V}{42.735}\right), \tag{1}$$

where D is the drought factor in the range 0 to 10, H is the relative humidity in percent, T is the air temperature in degrees Celsius, and V is the average wind speed at 10 m above the ground in the open, expressed in km h^{-1}. Though this expression can be used to evaluate the forest fire danger index at any time of day, normal practice is to calculate a daily value of F based on the maximum temperature and wind speed, and the minimum relative humidity.

The drought factor is a step variable derived from a drought index, I, (in mm equivalent), by (Noble *et al.*, 1980),

$$D = \frac{0.191(I + 104)(N + 1)^{1.5}}{3.52(N + 1)^{1.5} + R - 1}, \tag{2}$$

where N is the number of days since rain and R, in mm, is the sum of the last set of previously recorded non-zero 24-hour precipitation.

The drought index, I, represents the amount of daily rainfall (in mm) required to bring the soil to a field capacity (the water content at which internal drainage ceases) of 200 mm. The method of Keetch and Byram (1968), with the corrections noted by Alexander (1992), is used to calculate I. This uses a daily rainfall budget to estimate the water gain combined with an empirical relationship for daily water loss.

An annual measure of the forest fire danger is the cumulative annual forest fire danger index, which will be noted by ΣF. It is obtained by summing the daily values of F over the year. It is useful for a number of reasons. Because the dates of the bushfire season vary for different parts of Australia, and because of the possibility of out-of-season fires, the use of ΣF provides a basis with which to compare the fire danger of different sites. Another reason for its utility is that the probability distribution of the daily forest fire danger index is found to be exponentially distributed (Gill *et al.*, 1987). Thus knowledge of the cumulative index ΣF provides information on the mean value, and on the probability of occurrence of days of extreme fire danger.

3. Data

Descriptions of the CSIRO general circulation models are given by Gordon and Hunt (1987) and McGregor *et al.* (1993). The global models were run at 30 minute time steps and stored daily meteorological predictions over the Australia landmass for the following variables:

- Total precipitation at surface
- Mean surface humidity
- Maximum, minimum and mean surface air temperatures
- Maximum, minimum and mean surface temperatures
- Mean zonal and meridional winds at 900 hPa (CSIRO4) and 970 hPa (CSIRO9)
- Mean soil moisture (over the top 12 cm of soil).

The models were then run in equilibrium experiments with a doubled CO_2 atmosphere. The daily values of the above meteorological variables for the grid point which lies close to Sale (38°06′S, 147°08′E) were examined in detail.

The forest fire danger index is based on temperature and relative humidity at screen height (2 m) and on wind at a height of 10 m. The variables obtained from the model runs therefore had first to be manipulated.

3.1. TEMPERATURES

The lowest level in CSIRO4 is at 900 hPa, which corresponds to a height of about 1000 m. This GCM also produces a 'surface air temperature' that is obtained from the conservation of moist static energy through the lowest level (Gordon, 1981) and though it corresponds to the temperature at some height that is significantly greater than screen height, it has been used as a measure of screen temperature. The nine-level model (CSIRO9) directly produces temperatures at screen height by an interpolation method.

3.2. RELATIVE HUMIDITY

Fire danger index calculations are normally done on the minimum relative humidity for the day – i.e., the 3 pm weather readings. This was estimated by calculating the

dewpoint temperature from the mean temperature and the mean relative humidity, then using this dewpoint and the maximum temperature to estimate the minimum relative humidity. Using this method the dewpoint temperature is slightly lower than if it were calculated directly from the maximum temperature.

3.3. WIND

The GCMs generate winds on the basis of topography and the nature of the bottom boundary. There are two factors to incorporate into the wind speed. As mentioned above, an estimate of the maximum wind, rather than the mean wind, is needed. Secondly an estimate of the 10 m wind is needed. On the basis of Rossby similarity theory (McBean, 1979), the 10 m wind has a speed that is approximately 0.2 of the 900 hPa wind (Garatt, *pers. comm.*), and this correction factor was used.

There is considerable evidence (Beer, 1990) that the statistical distribution appropriate for hourly winds is a Rayleigh distribution (i.e. a Weibull distribution with a Weibull parameter of 2.0). The fifth percentile of a Rayleigh distribution has a value equal to 1.9 times the mean value. The fifth percentile is just slightly below the highest hourly wind. Accordingly, the daily mean wind (the only wind variable actually stored during the model runs) was multiplied by a factor of 2 to estimate the maximum hourly wind.

4. Results for Sale, Victoria

4.1. PRESENT CLIMATE

Beer *et al.* (1988) present a detailed analysis of behaviour of the fire weather variables responsible for the fire danger index at Sale, in Victoria. Using angle brackets to denote the mean, the mean climatic variables for Sale, based on 30 years of observations, are presently given in Table I, and denoted by $\langle\ \rangle$. By contrast, the relevant variables for the GCM 'control' ($1 \times CO_2$) simulations at the grid point closest to Sale are also given in Table I, with $\langle 4 \rangle$ indicating the four-level model results, and $\langle 9 \rangle$ indicating the nine-level model results.

It may be seen that for this grid point the GCM predictions for mean temperature, relative humidity and wind speed are all below those actually observed, whereas the rainfall is higher in the case of CSIRO4, and lower in the case of CSIRO9. Beer *et al.* (1988) point out that the single climatic parameter with the greatest influence on F on an annual basis is relative humidity, $H_{\min}$. A linear regression relates them by:

$$\Sigma F = -124.1\langle H_{\min} \rangle + 8603\,. \tag{3}$$

The GCM predictions for relative humidity are lower than those actually observed and hence, not surprisingly, the estimates for ΣF are higher than those actually observed. Figure 1 graphs the relationships between annual average minimum relative humidity and ΣF. The 41 years of meteorological data are shown as solid boxes. The line is the linear regression of humidity and fire danger index given in

TABLE I

Climatological results $\langle\,\rangle$ for Sale and GCM results for present climate ($\langle 4\rangle$ and $\langle 9\rangle$) and for a doubled CO_2 scenario ($\langle 4'\rangle$ and $\langle 9'\rangle$)

	Absolute						
	$\langle T\rangle$	$\langle T_{max}\rangle$	T_{max}	$\langle H_{min}\rangle$	$\langle V\rangle$	ΣR	ΣF
	C	C	C	%	km/h	mm	
$\langle\,\rangle$	13.7	18.9	44.0	54.9	23.6	612	1773
$\langle 4\rangle$	12.4	18.9	34.6	43.8	11.1	831	1958
$\langle 9\rangle$	13.6	20.2	37.1	27.7	9.4	357	3730
$\langle 4'\rangle$	17.0	23.6	40.9	39.7	10.6	799	3035
$\langle 9'\rangle$	19.0	25.2	42.2	27.3	9.6	396	4547

Equation 3. The scatter is, presumably, due to the fluctuations in precipitation, wind speed and temperature that are also important variables influencing fire danger.

Despite the unrealistic relative humidity results, the values generated by CSIRO4 for ΣF span the values of ΣF observed over the last forty years. The CSIRO4 model for this grid point is drier (i.e. lower relative humidity), but less windy and it would appear that the compensating effects of these two variables produce estimates for ΣF that are in accord with those presently observed. The nine-level model is far too dry at the grid point corresponding to Sale hence the fire danger is overpredicted. Nevertheless, the same general relationship between fire danger and relative humidity appears in both models and in the data.

4.2. DOUBLED CO_2

Outputs from GCMs simulating present and future climates should be used to determine changes in the variables rather than their absolute values. In the case of Sale, the doubled CO_2 results confirm the previous general relationship between relative humidity and forest-fire danger. The simulated relative humidity is lower and the value of ΣF is higher. In fact, as may be noticed in Figure 1, the predictions for the fire danger in the doubled CO_2 case all lie at the extreme upper limit of the presently occurring (or presently predicted) fire danger.

These results provide a degree of confidence in the results of the GCM model with respect to changes in fire danger index. The fire danger index variations in Figure 1 have increased by a little more than the amount one would expect on the basis of the humidity changes alone, but we believe this merely arises as a result of the statistical variability in the relationship between relative humidity and fire danger. We plan, in the future, to study this relationship at other grid points.

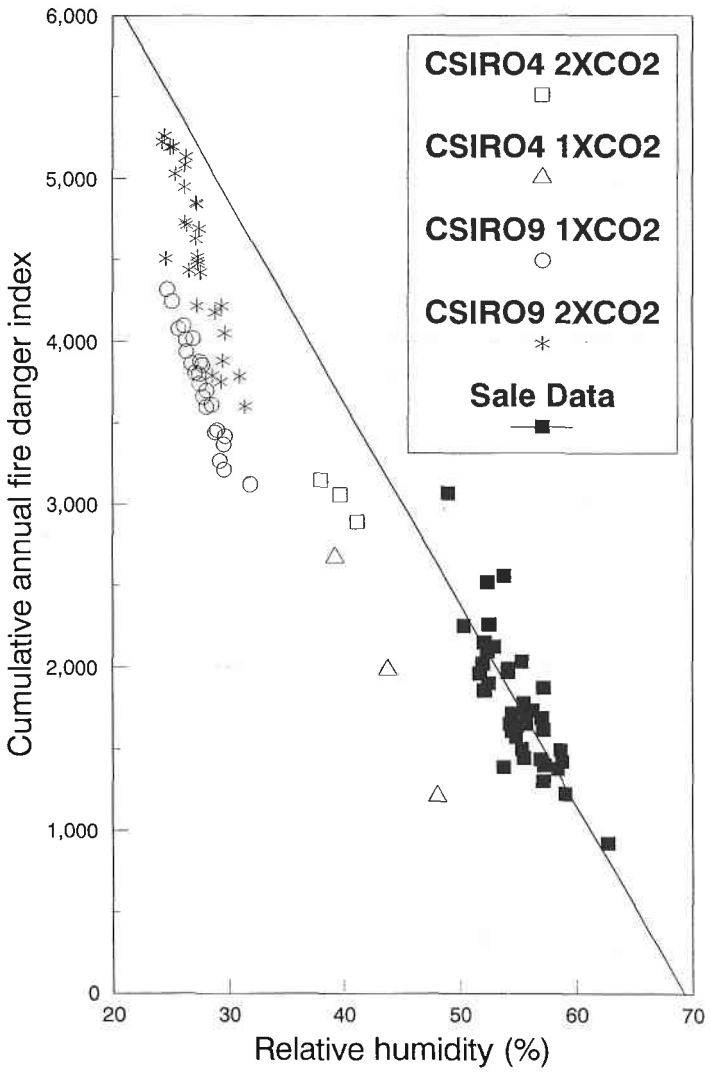

Fig. 1. Relationships between the annual average minimum relative humidity and ΣF for Sale, Victoria. Solid line is regression for existing data shown as filled rectangles. The points are the results of the GCM models for the present climate ($1 \times CO_2$ – triangles for CSIRO4, circles for CSIRO9) and for the climate that results from a doubling in CO_2 (open boxes for CSIRO4, asterisks for CSIRO9).

4.3. PROBABILITY DISTRIBUTION

The probability distribution of F, the daily forest fire danger index, is shown in Figures 2a and 2c for the CSIRO4 and CSIRO9 simulations of the present climate at the grid point nearest to Sale, and in Figures 2b and 2d for the simulation of the climate resulting from a doubling of CO_2. In a doubled CO_2 climate for this

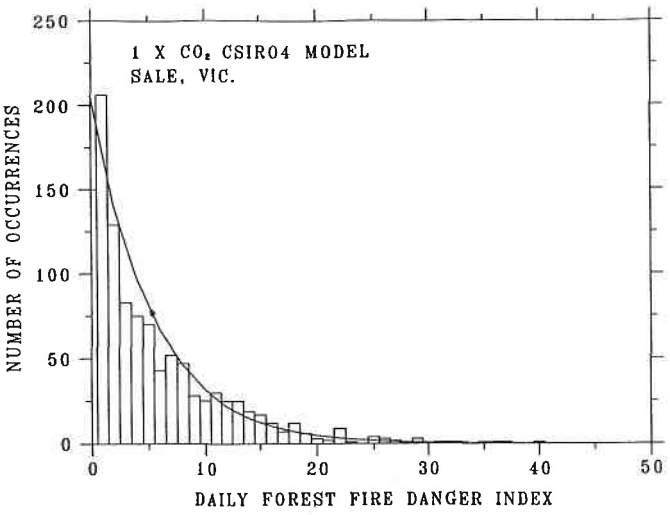

Fig. 2a.

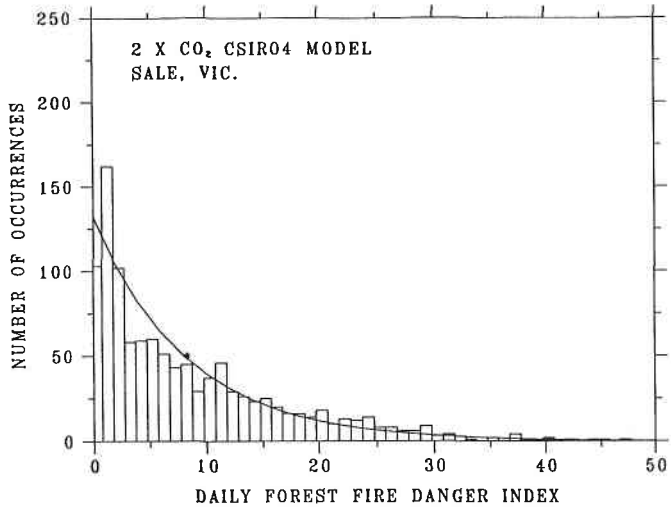

Fig. 2b.

location we expect fewer days of low fire danger and a greater proportion of days of high fire danger compared with the control climate.

The modelled results, especially the CSIRO4 results, display the same exponential dependence as that obtained by analysis of actual climatic data (Gill *et al.*, 1987). The solid lines in Figure 2 show the exponential fits to the data, with the asterisk marking the mean value of the daily forest fire danger index. The close correspondence between the exponential distribution, and the calculated daily values of F justifies the use of the annual summed forest fire danger index (ΣF) as a fire index. The reason is that the exponential distribution is a one-parameter

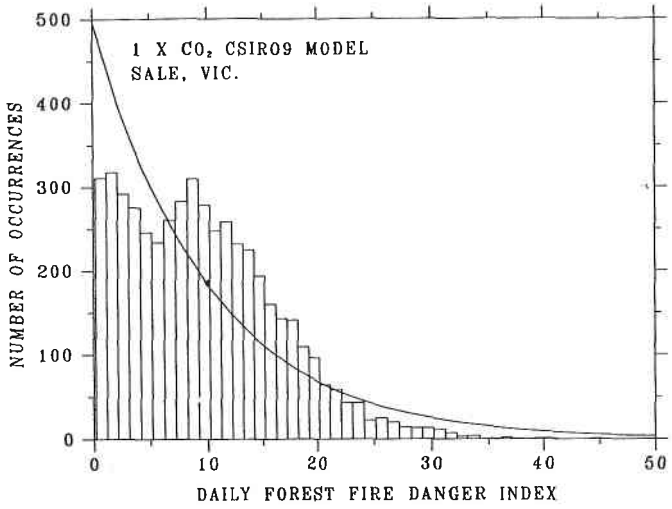

Fig. 2c.

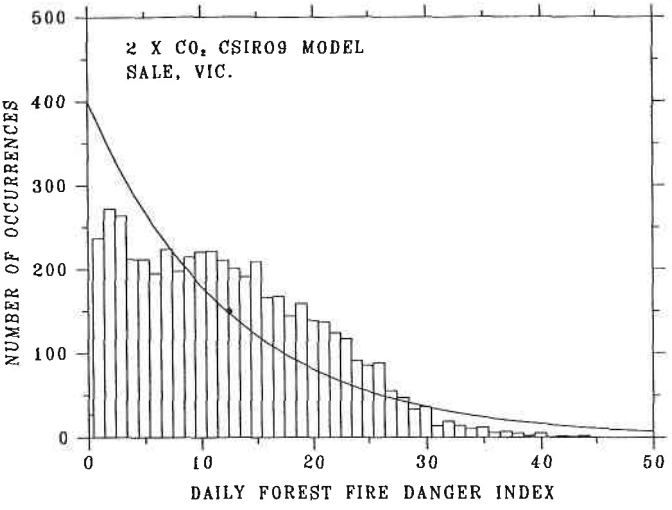

Fig. 2d.

Fig. 2. Probability distribution of the daily forest fire danger index, F, obtained from the grid point nearest Sale, Vic. for (a) three years simulation of the present ($1 \times CO_2$) climate from the CSIRO4 model; and from (c) thirty years simulation from the CSIRO9 model; and (b) the $2 \times CO_2$ climate of the CSIRO4 model; and (d) the CSIRO9 model. The solid line is an exponential fit to the distribution and the asterisk marks the mean value of F.

distribution so that knowledge of the mean ($\Sigma F/365$) – which is easily obtained from ΣF – is sufficient to completely specify the characteristics of the probability distribution.

The departure from the exponential distribution of the CSIRO9 results for Sale is most likely to be a result of the poor simulation of the model at this grid point. The grid point is too dry and the fire danger overpredicted which shows up in the probability distribution as fewer than expected low values, and more than expected of the medium to high values of fire danger.

5. Spatial Variation of Forest Fire Danger Index and Relative Humidity

Both the historical climatic data, and the results of the GCMs indicate that for Sale, Victoria the cumulative summed forest fire danger index and the annual mean of the daily minimum relative humidity are strongly negatively correlated. The question then arises as to whether this result is unique to this location or whether it is a general result applicable to the rest of Australia.

When the CSIRO4 model is run with a doubled CO_2 scenario, average annual relative humidities in the western, inland and south-eastern parts of Australia fall, and the fire danger rises. By contrast, the relative humidity in the north and north-eastern parts of Australia rises and the fire danger falls. The CSIRO9 results indicate a far more general decrease in relative humidity over most of Australia.

Figures 3a and 3b plot the changes in ΣF over Australia between the $1 \times CO_2$ and $2 \times CO_2$ climatic simulations of the CSIRO4 and CSIRO9 models. The main points to note in the case of the CSIRO4 model are that the western, inland and south-eastern parts of the continent are all predicted to have increased values of ΣF as a result of a doubling of CO_2. Coastal areas – especially in the north and north-east have decreased values of ΣF. Figures 4a and 4b plot the changes in the mean of the daily minimum relative humidity between the $1 \times CO_2$ and $2 \times CO_2$ climatic simulations of the CSIRO4 and CSIRO9 model. The general spatial distribution of the changes in relative humidity match the general spatial distribution of the changes in ΣF. Thus Figure 4a also shows decreases in relative humidity in the western, inland and south-eastern parts of the continent, along with increases in relative humidity in the north, north-east, and inland NSW. The correlation would be excellent in the case of the CSIRO4 model except for the small areas in the northern inland parts of the continent where both the relative humidity and fire danger increase.

The relationship between relative humidity and forest fire danger index is slightly weaker in the case of the CSIRO9 model, and this may be a result of the fact that the rainfall changes (and thus the humidity changes) are more seasonally dependent in the CSIRO9 model than in the CSIRO4 model.

6. Theory

The relative humidity change after a temperature increase arising from increased carbon dioxide levels is not intuitively obvious. The increase in temperature means that the saturated vapour pressure increases greatly, so that the atmosphere can

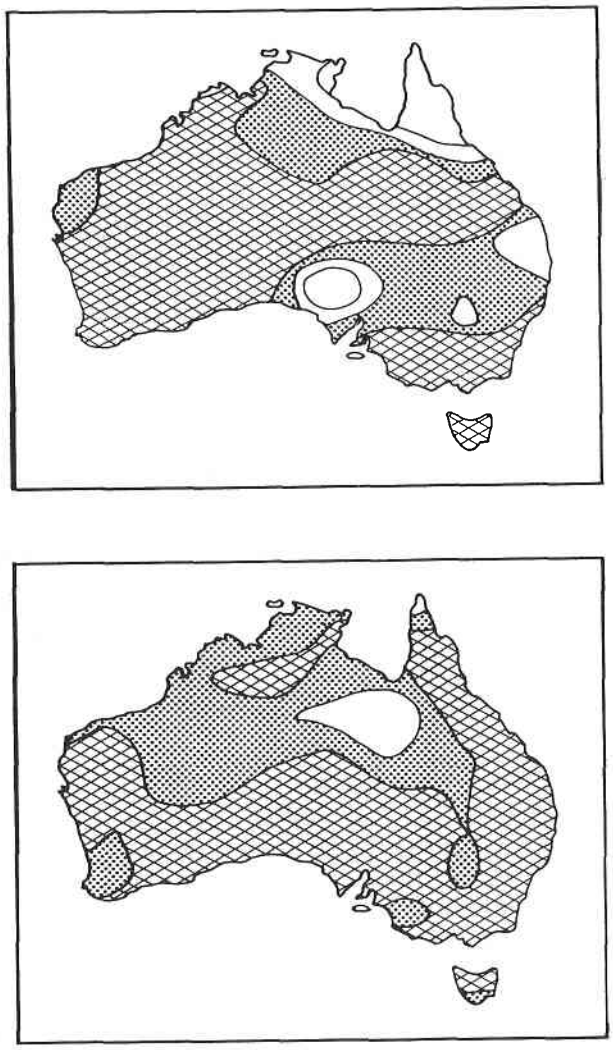

Fig. 3. Changes in ΣF over Australia between the $1 \times CO_2$ and $2 \times CO_2$ climatic simulations of the (a) CSIRO4 model; and (b) CSIRO9 model. The blank areas are regions of decreased ΣF, the spotted regions are increases of ΣF between 0 and 10%, and areas that are cross-filled have ΣF increasing by more than 10%.

hold more water, and therefore a lower relative humidity might be expected. But an increased temperature also increases the potential evaporation rate, so that a higher relative humidity could be expected if there is sufficient soil moisture for there to be an increase in the rate of actual evaporation. The problem is complex and the early generation of general circulation models postulated a constant relative humidity (Manabe and Wetherald, 1975), and this assumption occasionally continues to be used (e.g., Bultot *et al.*, 1988). Because of the close link between relative humidity

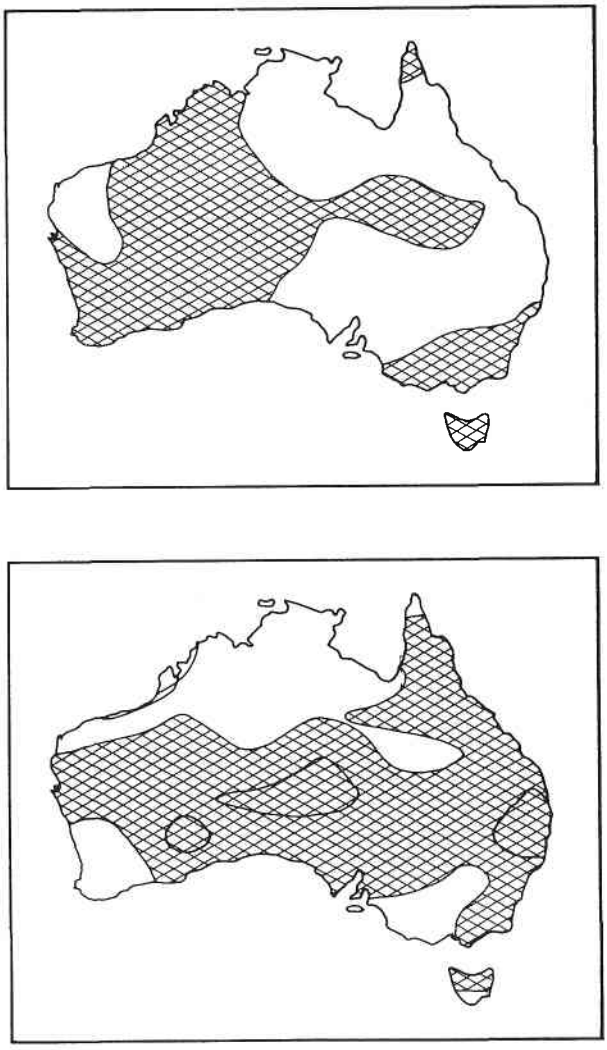

(a)

(b)

Fig. 4. Changes in the mean of the daily minimum relative humidity between the $1 \times CO_2$ and $2 \times CO_2$ climatic simulations of the (a) CSIRO4 model; and (b) CSIRO9 model. Cross filled areas are regions with decreased relative humidity, and blank areas are regions of increased relative humidity.

and forest fire danger, this is not an appropriate assumption to make when examining the likely incidence of fire danger under a changed climatic regime.

This section presents a one-box analytical-empirical model designed to provide a simplified insight into the conditions necessary for an increase or decrease in relative humidity, after a fixed change in air temperature (from T to T') as a result of a doubling of CO_2. Assume that there is an equilibrium between the existing actual evaporation, E_a, (over a surface of area A) and the water vapour as measured

by the mixing ratio r (within a box of height h). The combination method (Monteith, 1981) estimates potential evaporation into the box from:

$$\rho_w L E_p = \frac{s(R_n - G) + \rho_a c_p (e_s - e)/r_a}{s + \gamma}, \tag{4}$$

where R_n is the nett radiation, G is the soil heat flux, L is the latent heat of vaporization of water (2.47×10^6 J kg^{-1} at 15 °C), and E_p is the potential evaporation rate (in m s^{-1}). The density of water is ρ_w.

The air density is ρ_a, the term c_p is the specific heat of the air at constant pressure, e is the vapour pressure at the fuel (assumed to be the same as that at screen height), and e_s is the saturation vapour pressure of water vapour at fuel temperature (which is approximated by the air temperature). The polynomial expression of Sargent (1980) can be used to evaluate e_s. The term r_a is the aerodynamic resistance (assumed the same for the resistance to heat transport and vapour transport), γ is the psychrometric constant, and s is the derivative of the saturation vapour pressure with respect to temperature.

Under a new climatic regime, a new evaporative equilibrium will be established, characterised by an evaporation E'_a. This change in actual evaporation results in a change in the mixing ratio (to r'). Applying mass conservation we find

$$r' V_b \rho_a = r V_b \rho_a + (E'_a - E_a)\rho_w A \tau, \tag{5}$$

where V_b is the volume of the box, ρ_w is the density of water, and τ is the length of time required to attain the new equilibrium. Because $r \simeq 0.622 e/p$

$$e' = e + 1.61 p \rho_w (E'_a - E_a)\tau/(h\rho_a), \tag{6}$$

where p is the atmospheric pressure. The relative humidity changes from e/e_s to e'/e'_s, where $e'_s = e_s(T')$. Equation 4 and 6, when taken together, provide a means of estimating changes in relative humidity subject to (i) parameterisation of the terms in the two equations; and (ii) a relationship between E_p and E_a.

6.1. PHYSICAL VARIABLES

Changes in water vapour influence the formation of clouds that can then affect the nett solar radiation such that it increases or decreases according to the height and the optical thickness of the resulting clouds. To maintain the simplicity of the one-box model we assume that the nett solar radiation and soil heat flux remain unchanged.

The aerodynamic resistance, r_a, for a neutrally stable atmosphere, is (Thom and Oliver, 1977)

$$r_a = \frac{4.72}{(1 + 0.54u)} \left[\ln\left(\frac{z}{z_0}\right)\right]^2, \tag{7}$$

where the reference height for anemometry used to calculate Equation 7 is $z = 10$ m and where the roughness length, $z_0 = 1.37$ mm for open water surfaces (Thom and

Oliver, 1977, p. 351). The wind speed, u, is in m s^{-1} and refers to the daily mean value obtained at 10 m height. As discussed in section 3.3, $\langle u \rangle = \langle V \rangle / 2$.

The term, τ is taken to correspond to the time scale for vertical tropospheric mixing of water vapour. An indication of its value may be obtained from residence time estimates where τ has a value that ranges between 9 and 13 days (Brutsaert, 1982, p. 5), so that a value of 10 days is taken as being appropriate. This time is assumed to remain unchanged under doubled CO_2 conditions.

The vertical distribution of saturated vapour pressure can be derived from the Clausius-Clapeyron equation as:

$$\frac{de_s}{dz} = \frac{M_v L e_s}{RT^2} \frac{dT}{dz} \tag{8}$$

where M_v is the molar mass of water vapour (18 g mol^{-1}) and L is the latent heat of vaporization of water. For a dry adiabatic lapse rate of $dT/dz = -9.8$ K km^{-1} substitution into Equation 8 for 15 °C indicates $e_s/(de_s/dz)$ has a value of about 1.6 km. The fractional rate of decrease in vapour pressure with height is about five times greater than the corresponding fractional rate of decrease in total pressure. Climatological data (Lorenz, 1967, p. 42) indicate that specific humidity has an approximately exponential distribution for which a scale height of 1.6 km is reasonable.

6.2. RELATIONSHIP BETWEEN E_p AND E_a

The relationship between the actual and potential evaporation for Australia has been estimated by using the results of the CSIRO9 model (under the $1 \times CO_2$ simulation) as surrogates for E_a, and the contours of evaporation measured from Australian sunken tanks (Bureau of Meteorology, 1968) (E_s) as surrogates for E_p. The relationship between the two, for points on the grid comprising the CSIRO9 model, is given in Figure 5.

The points depicted in Figure 5 have been fitted by the solid line:

$$\rho_w L E_a = 74.6 - 0.24 \rho_w L E_s \,, \tag{9}$$

where the parameter values were chosen using a linear regression package. The form of Equation 9 illustrates two points. In the first place it was noticed that within Australia there is an inverse relationship between E_a and E_s. This is because locations with the highest potential evaporation occur in desert regions of the centre of the country where the actual evaporation is low, whereas regions along the south-eastern Australian coasts with high actual evaporation have relatively low potential evaporation rates. Secondly, though there is a general requirement that $E_a < E_p$, so that at high values of E_a the inverse relationship must cease and be replaced by a linear relationship, the results indicate that actual evaporation rates over land are never sufficiently high that Equation 9 needs to be replaced by a functional relationship that increases E_s as E_a increases.

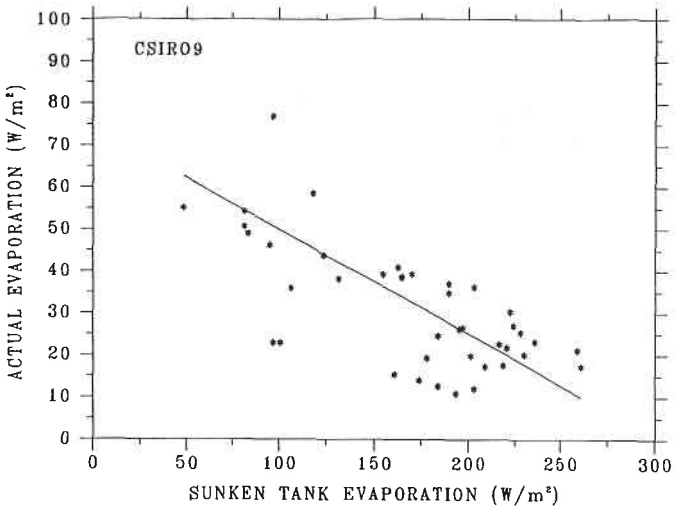

Fig. 5. Deduced relationship between potential and actual evaporation where Australian sunken tank measurements are used as surrogates for potential evaporation and modelled results are used as surrogates for actual evaporation. 100 W/m^2 over a year corresponds to an evaporation of 1.31 m of water, or 3.6 mm/day.

The relationship between E_s and E_p requires the incorporation of a pan coefficient to allow for the evaporation measured in a finite sized evaporation pan being higher than that measured in an open body of water under the same meteorological conditions. Based on results in Australian Water Resources Council (1970), the pan coefficient for the now obsolete Australian sunken tank is about 0.85 so that we use:

$$E_p = 0.85E_s \,. \tag{10}$$

Because we have no basis for relating potential and actual evaporation under an altered climatic regime, Equation 9 is used to link potential and actual evaporation for both the present and the altered climate.

7. Discussion

The expected change in relative humidity can be found by using Equations 4, 6 and 10, when parameterised as above. This depends primarily on the current values of the relative humidity and the evaporation rate, but is also dependent on the likely change in wind speed. Appendix 1 discusses the changes to be expected as a result of these factors.

When Equation 9 is used, which is appropriate to the results of the CSIRO9 model, then the relative humidity as a result of a warming always decreases. To illustrate that there are situations in which relative humidity may either decrease

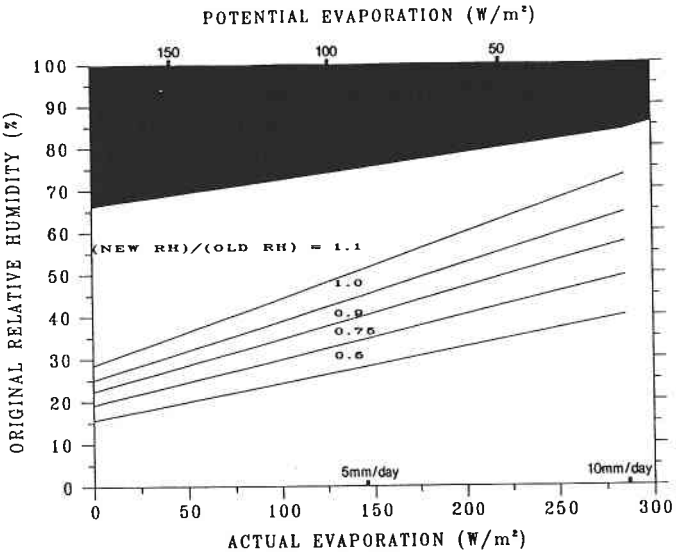

Fig. 6. Predicted changes in relative humidity (using the simple one-box model) following a warming from 15 °C to 19 °C and a decrease in mean wind speed from 11.7 km h^{-1} (3.25 m s^{-1}) to 7.2 km h^{-1} (2 m s^{-1}). The relation between actual and potential evaporation resulting from the CSIRO4 data has been used. Solid lines mark constant ratios of new to original relative humidity. The shaded region corresponds to predictions of greater than 100%. The predictions use the combination equations and assume that the characteristic speed of the vertical flux of water vapour, h/τ, is 0.16 km/day.

or increase we have used the CSIRO4 results. The equivalent relationship for the CSIRO4 model was:

$$\rho_w LE_a = 334.3 - 1.71\rho_w LE_s \,. \tag{11}$$

Figure 6 uses Equation 11 to depict the change in relative humidity (expressed as a ratio) associated with a representative greenhouse warming from an average temperature of 15 °C to 19 °C, and a decrease in the mean wind speed from 11.7 km h^{-1} (3.25 m s^{-1}) to 7.2 km h^{-1} (2 m s^{-1}). The temperature change is representative of that expected in south-eastern Australia, whereas the mean wind speed is one half of the mean daily maximum wind speed observed at Sale (section 4.1). The reason for the chosen decrease is given in Appendix 1. The simple one-box model predicts that regions such as central Australia with low relative humidity will decrease in relative humidity, whereas mid-latitude coastal regions with high relative humidity will increase in relative humidity (provided that the wind speed decreases). If the mean wind speed remains unchanged or is decreased by only a small amount then, as indicated in the sensitivity analysis of Appendix 1, the relative humidity increases for all realistic evaporation rates associated with the CSIRO4 model, but decreases for all realistic evaporation rates associated with the CSIRO9 model.

The behaviour shown in Figure 6 and discussed above agrees with the general CSIRO4 results when examined for relative humidity and evaporation. At the extreme corners of the diagram, points with low actual evaporation rate and high relative humidity show an increase in relative humidity, whereas points with high actual evaporation and low relative humidity show a decrease in relative humidity. Similarly, there is a tendency for most points in the CSIRO9 model to display a decrease in relative humidity. As our one-box analysis shows, the slope of the curve linking actual and potential evaporation (represented as μ in Appendix 1) plays a key role in determining the expected response of fire danger to climatic change, because it plays a key role in determining the relative humidity changes. Because there are so few measurements of actual evaporation, it is necessary to use the results of GCMs to estimate actual evaporation. This highlights the fact that a realistic representation of the hydrological cycle is needed in a GCM before it can be expected to provide a reasonable representation of the fire danger. In this respect, the CSIRO9 model provides a better simulation than the CSIRO4 model of the rainfall over most of Australia (Whetton *et al.*, 1993) – though the grid point corresponding to Sale happens to be anomalous in producing rainfall predictions that do not agree well with observations.

Shuttleworth (1983) has examined the response of evaporation to changes in climatic variables. He makes the point that the evaporative response to climatic change is complicated by the fact that meteorological variables influencing evaporation may realistically be expected to change in a related way. Moreover, present-day vegetation is strongly linked to prevailing climate and, therefore, will alter in response to major, long-term climatic change, particularly changes in temperature and precipitation. Thus general observations can be made only in regard to small-scale or short-term climatic change in which the type of vegetation prevalent at the location of interest does not alter significantly. However, fire plays a major role in initiating vegetation succession and atmospheric humidity plays a major role in determining the likely fire danger. There is therefore a need to discuss the effects of climatic change on evaporation and humidity by assuming that the vegetation remains unchanged, for it is only through such discussions that we can start to estimate the direction and rate at which vegetation change will proceed.

8. Conclusions

The results of the general circulation models used in this study indicate that climatic change, caused by increased CO_2, could change the expected value of the Australian forest fire danger index, F. When evaluated over a complete year, changes in F are primarily controlled by changes to the relative humidity. This observation, originally made by Beer *et al.* (1988) on the basis of historical meteorological data collected at sites in eastern Australia, appears to be true over much of the continent. A simple one-box model of evaporation then indicates that whether the relative humidity change is positive or negative depends on:

- the relationship between actual and potential evaporation;
- the expected changes in the wind speed;
- the present value of the relative humidity; and
- the present value of the evaporation rate.

The estimate of the relationship between actual and potential evaporation that was obtained using the CSIRO9 model (considered to be more reliable than that obtained from CSIRO4) predicts that relative humidity always decreases as a result of a warming. This implies a widespread increase in the forest fire danger index over Australia as a result of enhanced greenhouse warming, and this is indeed the result obtained from the CSIRO9 model as depicted in Figure 3b.

Appendix 1 – Sensitivity Analysis of the One-Box Model

We retain the same symbols as before and generalise the equations to be solved as:

$$e' = e + \alpha(E'_{\mathrm{a}} - E_{\mathrm{a}})$$

$$E_{\mathrm{a}} = C - \mu E_{\mathrm{p}} ,$$

so that

$$e' = e + \mu\alpha(E_{\mathrm{p}} - E'_{\mathrm{p}}) , \tag{A1}$$

whereas the combination equation gives:

$$\beta E_{\mathrm{p}} = sQ + f(e_{\mathrm{s}} - e) \tag{A2}$$

$$\beta' E'_{\mathrm{p}} = s'Q' + f'(e'_{\mathrm{s}} - e') . \tag{A3}$$

It is assumed that $Q = Q'$. An expression for e' is obtained by eliminating Q from A2 and A3, and then eliminating E'_{p} from the resulting equation by using A1. This yields:

$$(\lambda - f's)e' = (\lambda - fs')e + fs'e_{\mathrm{s}} - f'se'_{\mathrm{s}} - (\beta s' - \beta' s)E_{\mathrm{p}} , \tag{A4}$$

where:

$$\lambda - \beta' s/(\mu\alpha) .$$

The new relative humidity, H', is then found as:

$$\begin{aligned} (\lambda - f's)H' &= (\lambda - f's)\frac{e'}{e'_{\mathrm{s}}} \\ &= \zeta(\lambda - fs')H + \zeta fs' - f's - (\beta s' - \beta' s)\left(\frac{E_{\mathrm{p}}}{e'_{\mathrm{s}}}\right) , \end{aligned}$$

where:

$$\zeta = \frac{e_s}{e'_s} .$$

The numerical values used in the one-box model (assuming the evaporation rates are in W m^{-2}) are: $\alpha = 0.294$, $\beta = 1.75$, $\beta' = 2.03$, $s = 1.095$, $s' = 1.37$, $e_s = 17$, $e'_s = 22$, $f = 8.9$ so that $\zeta = 0.77$ and $\lambda = 3.7$.

If it is assumed that the mean wind does not vary then f remains constant. If these values are used with a value of $\mu = 0.28$, as inferred from the link between the actual and potential evaporation results of the CSIRO9 model then H' is always less than H. The CSIRO4 results indicated a much higher value of $\mu = 2.0$ in which case H' is always greater than H. The results depicted in Figure 7, that indicate that H' can be either greater or less than H, depending on the original relative humidity and evaporation rate, were obtained by assuming a decrease in wind so that $f' = 6.7$, and a value of $\mu = 2.0$, appropriate to the CSIRO4 model. When the value of $\mu = 0.28$ appropriate to the CSIRO9 model is used then the one-box model continues to predict that the relative humidity decreases virtually irrespective of the original humidity and evaporation rate.

References

Alexander, M. E.: 1992, 'The Keetch-Byram Drought Index: A Corrigendum', *Bull. Am. Met. Soc.* **73**, 61.

Australian Water Resources Council: 1970, *Evaporation from Water Storages*, Hydrological Series No. 4, Department of National Development, Canberra, Australia.

Balling, R. C., Jr., Meyer, G.A., and Wells, S. G.: 1992, 'Climate Change in Yellowstone National Park: Is the Drought Related Risk of Wildfires Increasing?', *Clim. Change* **22**, 35–45.

Beer, T.: 1990, *Applied Environmetrics Meteorological Tables*, Applied Environmetrics, Balwyn, p. 46.

Beer, T.: 1991a, *Applied Environmetrics Hydrological Tables*, Applied Environmetrics, Balwyn, pp. 40–44.

Beer, T.: 1991b, 'The Interaction of Wind and Fire', *Bound. Layer Met.* **54**, 287–308.

Beer, T., Gill, A. M., and Moore, P. H. R.: 1988, 'Australian Bushfire Danger under Changing Climatic Regimes', in Pearman, G. I. (ed.), *Greenhouse: Planning for Climatic Change*, CSIRO, pp. 421–427.

Brutsaert, W. H.: 1982, *Evaporation into the Atmosphere*, Reidel, Dordrecht.

Bultot, F., Dupriez, G. L., and Gellens, D.: 'Estimated Annual Regime of Energy-Balance Components, Evapotranspiration and Soil Moisture for a Drainage Basin in the Case of a CO_2 Doubling', *Clim. Change* **12**, 39–56.

Bureau of Meteorology (for Australian Water Resources Council): 1968, *Review of Australia's Water Resources: Monthly Rainfall and Evaporation – Part 2, Maps*, Bureau of Meteorology, Melbourne.

Fried, J. S. and Torn, M. S.: 1990, 'Analyzing Localized Climate Impacts with the Changed Climate Fire Modeling System', *Natur. Resource Model.* **4**, 229–253.

Gill, A. M., Christian, K. R., Moore, P. H. R., and Forrester, R. I.: 1987, Bushfire Incidence, Fire Hazard and Fuel Reduction Burning', *Aust. J. Ecol.* **12**, 299–306.

Gordon, H. B. and Hunt, B. G.: 1987, 'Interannual Variability of the Simulated Hydrology in a Climatic Model – Implications for Drought', *Clim. Dynam.* **1**, 113–130.

Gordon, H. B.: 1981, 'A Flux Formulation of the Spectral Atmospheric Equations Suitable for Use in Long-Term Climate Modelling', *Mon. Wea. Rev.* **109**, 54–56.

Keetch, J. J. and Byram, G. M.: 1968, 'A Drought Index for Forest Fire Control', *USDA Forest Service Research Paper* SE-38, Asheville, North Carolina (reprinted with corrections in 1988).

Lorenz, E. N.: 1967, 'The Nature and Theory of the General Circulation of the Atmosphere', World Meteorological Organization, Geneva.

Manabe, S. and Wetherald, R. T.: 1975, 'The Effects of Doubling the CO_2 Concentration on the Climate of a General Circulation Model', *J. Atmos. Sci.* **32**, 3–15.

McArthur, A. G.: 1966, 'Weather and Grassland Fire Behaviour', *Commonw. Aust. For. Timber Bur. Leaflet* **100**.

McArthur, A. G.: 1967, 'Fire Behaviour in Eucalypt Forest', *Commonw. Aust. For. Timber Bur. Leaflet* **107**.

McBean, G. A.: 1979, *The Planetary Boundary Layer*, Technical Note 165, World Meteorological Organization, Geneva, p. 42.

McGregor, J. L., Gordon, H. B., Watterson, I. G., Dix, M. R. and Rotstayn, L. D.: 1993, *The CSIRO 9-Level Atmospheric General Circulation Model*, Technical Paper 26, Division of Atmospheric Research, CSIRO, Australia.

Monteith, J. L.: 1981, 'Evaporation and Surface Temperature', *Q. J. Roy. Met. Soc.* **107**, 1–27.

Noble, I. R., Bary, G. A. V., and Gill, A. M.: 1980, 'McArthur's Fire-Danger Meters Expressed as Equations', *Aust. J. Ecol.* **5**, 201–203.

Robertson, G. W.: 1983, *Weather-Based Mathematical Models for Estimating the Development and Ripening of Crops*, Technical Note No. 180, (WMO-# 620), World Meteorological Organization, Geneva.

Sargent, G. P.: 1980, 'Computation of Vapour Pressure, Dew Point and Relative Humidity from Dry and Wet Bulb Temperatures', *Met. Mag.* **109**, 238–246.

Shuttleworth, W. J.: 1983, 'Evaporation Models in the Global Water Budget', in Street-Perrott, A. *et al.* (eds.), *Variations in the Global Water Budget*, D. Reidel Publishing Co., Dordrecht, pp. 147–171.

Thom, A. S. and Oliver, H. R.: 1977, 'On Penman's Equation for Estimating Regional Evaporation', *Q. J. Roy. Met. Soc.* **103**, 345–357.

Torn, M. S. and Fried, J. S.: 1992, 'Predicting the Impacts of Global Warming on Wildland Fire', *Clim. Change* **22**, 257–274.

Whetton, P. and Pittock, A. B.: 1991, *Australian Region Intercomparison of the Results of Some General Circulation Models Used in Enhanced Greenhouse Experiments*, Tech. Paper 21, CSIRO Division of Atmospheric Research, Aspendale, Vic.

Whetton, P. H., Fowler, A. M., Haylock, M. R., and Pittock, A. B.: 1993, 'Implications of Climate Change Due to the Enhanced Greenhouse Effect on Floods and Droughts in Australia', *Clim. Change* **25**, 289–317.

Whetton, P. H., Rayner, P. J., Pittock, A. B., and Haylock, M. R.: 1994, 'An Assessment of Possible Climate Change in the Australian Region Based on an Intercomparison of General Circulation Modelling Results', *J. Clim.* **7**, 441–463.

(Received 10 December, 1993; in revised form 26 July, 1994)